CRIP1 involves the pathogenesis of multiple myeloma via dual-regulation of proteasome and autophagy

Peixia Tang,[a,b,e] Zhen Yu,[a,b,e] Hao Sun,[a] Lanting Liu,[a,b] Lixin Gong,[a] Teng Fang,[a] Xiyue Sun,[a] Shiyi Xie,[a] Gang An,[a] Zhenshu Xu,[c,***] Lugui Qiu,[a,b,d,**] and Mu Hao[a,b,*]

[a]State Key Laboratory of Experimental Hematology, National Clinical Research Center for Blood Diseases, Haihe Laboratory of Cell Ecosystem, Institute of Hematology & Blood Diseases Hospital, Chinese Academy of Medical Sciences & Peking Union Medical College, Tianjin, China
[b]Tianjin Institutes of Health Science, Tianjin, China
[c]Hematology Department Fujian Medical University Union Hospital, Fujian Institute of Hematology, Fuzhou, Fujian, China
[d]Gobroad Healthcare Group, Beijing, China

eBioMedicine
2024;100: 104961
Published Online xxx
https://doi.org/10.1016/j.ebiom.2023.104961

Summary

Background Multiple myeloma (MM) is an incurable hematological malignancy of the plasma cells. The maintenance of protein homeostasis is critical for MM cell survival. Elevated levels of paraproteins in MM cells are cleared by proteasomes or lysosomes, which are independent but inter-connected with each other. Proteasome inhibitors (PIs) work as a backbone agent and successfully improved the outcome of patients; however, the increasing activity of autophagy suppresses the sensitivity to PIs treatment.

Methods The transcription levels of CRIP1 were explored in plasma cells obtained from healthy donors, patients with newly diagnosed multiple myeloma (NDMM), and relapsed/refractory multiple myeloma (RRMM) using Gene expression omnibus datasets. Doxycycline-inducible CRIP1-shRNA and CRIP1 overexpressed MM cell lines were constructed to explore the role of CRIP1 in MM pathogenesis. Proliferation, invasion, migration, proteasome activity and autophagy were examined in MM cells with different CRIP1 levels. Co-immunoprecipitation (Co-IP) with Tandem affinity purification/Mass spectrum (TAP/MS) was performed to identify the binding proteins of CRIP1. The mouse xenograft model was used to determine the role of CRIP1 in the proliferation and drug-resistance of MM cells.

Findings High CRIP1 expression was associated with unfavorable clinical outcomes in patients with MM and served as a biomarker for RRMM with shorter overall survival. In vitro and in vivo studies showed that CRIP1 plays a critical role in protein homeostasis via the dual regulation of the activities of proteasome and autophagy in MM cells. A combined analysis of RNA-seq, Co-IP and TAP/MS demonstrated that CRIP1 promotes proteasome inhibitors resistance in MM cells by simultaneously binding to de-ubiquitinase USP7 and proteasome coactivator PA200. CRIP1 promoted proteasome activity and autophagosome maturation by facilitating the dequbiquitination and stabilization of PA200.

Interpretation Our findings clarified the pivotal roles of the CRIP1/USP7/PA200 complex in ubiquitin-dependent proteasome degradation and autophagy maturation involved in the pathogenesis of MM.

Funding A full list of funding sources can be found in the acknowledgements section.

Keywords: Multiple myeloma; PIs resistance; CRIP1; Autophagy; Proteasome degradation

*Corresponding author. State Key Laboratory of Experimental Hematology, National Clinical Research Center for Blood Diseases, Institute of Hematology & Blood Diseases Hospital, No. 288 Nanjing Road, Tianjin, 300020, China.
**Corresponding author. State Key Laboratory of Experimental Hematology, National Clinical Research Center for Blood Diseases, Institute of Hematology & Blood Diseases Hospital, No. 288 Nanjing Road, Tianjin, 300020, China.
***Corresponding author. Hematology Department Fujian Medical University Union Hospital, Fujian Institute of Hematology, No. 29 Xinquan Road, Fuzhou, Fujian, 350001, China.
E-mail addresses: haomu@ihcams.ac.cn (M. Hao), qiulg@ihcams.ac.cn (L. Qiu), xuzs@fjmu.edu.cn (Z. Xu).
[e]These authors contributed equally.

Research in context

Evidence before this study

Although proteasome inhibitors (PIs) have transformed management of multiple myeloma (MM), drug resistance emerges through induction of the aggresome & autophagy pathway as a compensatory protein clearance mechanism. Accordingly, autophagy inhibitors used in association to conventional anti-MM drugs might enforce the effect against resistant MM cells and render autophagy a new therapeutic target. Our previous study identified that CRIP1 was a high-risk gene that overexpressed in drug-resistance MM cells in post-treatment patient samples. However, the molecular mechanism of CRIP1 contribute to PIs resistance has not been fully understood.

Added value of this study

In this study, we evaluated the mechanism of CRIP1-mediated PIs resistance and MM cell aggressive proliferation. Our data showed that CRIP1 was overexpressed in MM cells in patients with RRMM (relapsed/refractory MM). CRIP1 overexpression is linked to inferior outcome in patients with MM even those undergoing bortezomib (BTZ) treatment. CRIP1 promoted MM cell proliferation, invasion, and decreased PIs sensitivity in MM cells. More important, CRIP1 overexpression stabilized PA200 and against PIs induced MM cell apoptosis by enhancing the proteasome activity and autophagy. Co-IP and TAPMS analysis indicated that CRIP1 promoted the de-ubiquitination and stabilization of PA200 by binding with USP7. Strikingly, our study elucidated that CRIP1 and PA200 were both the substrates of USP7. CRIP1 worked as a scaffold protein and played critical roles in BTZ resistance by forming the complex with USP7 and PA200. In vitro and in vivo studies further confirmed that the USP7 or PSME4 inhibition reduces CRIP1 induced BTZ-resistance in MM.

Implications of all the available evidence

Our study presented here demonstrated that CRIP1 was overexpressed in MM cells and correlated with inferior outcome of MM patients. CRIP1 facilitated proteasome activity and autophagy and induced the BTZ resistance of MM cells through promoting PA200 bind with USP7. Blocking CRIP1/USP7/PA200 signal pathway would be an ideal strategy for MM therapy which can suppress proteasome activity and autophagy simultaneously.

Introduction

Multiple myeloma, a cancer of the immunoglobulin-producing plasma cells, is exceptionally sensitive to death caused by proteasome inhibitors (PIs).[1] Protein homeostasis (proteostasis) is a highly complex and interconnected process used by cells to maintain concentration, conformation, and subcellular localization of proteins.[2] Many pathways are involved in controlling protein synthesis, folding, protein transport, and disposal.[3–5] In eukaryotic cells, damaged proteins or organelles can be cleared by proteasomes or lysosomes.[6] These two pathways are independent but interconnected with each other.[7] In general, proteasomes eliminate short-lived proteins and soluble misfolded proteins via the ubiquitin-proteasome system (UPS). In contrast, lysosomes are responsible for the degradation of long-lived proteins, insoluble protein aggregates, even entire organelles, macromolecular compounds, and intracellular parasites (e.g. certain bacteria) via endocytosis, phagocytosis, or autophagy pathways.[8,9] Over the past decade, PIs have become the therapeutic backbone of myeloma treatment. However, resistance to PIs in MM remains a challenge in clinical practice.[10,11] The mechanisms of PIs resistance in MM include the ubiquitin-proteasome pathway, autophagy-lysosome pathway, endoplasmic reticulum stress pathway, cell survival signal pathway,[5,12] exosome-mediated resistance,[13] and bone marrow microenvironment-mediated resistance.[13–17] Clarifying the molecular mechanisms of PIs resistance and determining the critical targets will benefit the potential therapeutic strategies for myeloma.

Cysteine-rich intestinal protein 1 (CRIP1), a member of the LIM/double zinc finger protein family, is abnormally expressed in several tumour types,[18] and plays critical roles in the growth and differentiation of eukaryotic cells.[19,20] However, limited data are available regarding the role of CRIP1 in cancer. He et al. Have reported that CRIP1 functions as an oncogene that regulate the migration and invasion of metastatic colorectal cancer (CRC). Moreover, CRIP1 facilitates homologous repair of chemotherapy-induced DNA damage in patients with gastric cancer (GC).[21] CRIP1 also affects the interactions of tumor cells with components of the immune system in patients with breast cancer[21,22] and is considered as a new biomarker for osteosarcoma, prostate cancer and breast cancer.[23] CRIP1 also acts as a clinical prognostic factor in patients with acute myeloid leukaemia (AML) with t[8,21] translocation.[24]

CRIP1 contains a cysteine-rich LIM domain that promotes protein–protein interactions and plays an important role in the ubiquitination-induced degradation of proteins. CRIP1 suppresses apoptosis and the chemosensitivity of 5-fluorouracil in CRC cells through ubiquitin-mediated Fas degradation.[25] CRIP1 also facilitates the interaction between the ubiquitin ligase STUB1 and carnitine synthesis enzyme BBOX1, enhancing BBOX1 ubiquitination and proteasomal degradation in hepatocellular carcinoma (HCC).[26] Hence, maintaining cellular protein homeostasis (proteostasis) is critical for the survival of MM cells, representing a fundamental biological characteristic of MM. Increased proteasome activity promotes drug-resistance to

PIs in MM, as reported in our previous study.[27] Therefore, we speculated that CRIP1 is involved in the regulation of proteostasis and promotes MM progression.

In this study, we evaluated the clinical significance of CRIP1 in patients with MM and investigated its pathophysiological functions, and the underlying molecular mechanisms in myeloma. Our findings suggested that CRIP1 plays a critical role in PIs resistance by binding to ubiquitin-specific protease 7 (USP7) and the proteasome activator PA200. High-level CRIP1 expression is an indicator of high-risk and drug-resistant MM that would benefit from adjuvant anti-USP7 or-PA200 therapy. CRIP1, as a potential therapeutic target in high-risk MM, promotes proteasome activity and autophagosome maturation in MM by stabilizing PA200.

Methods

Primary patient samples

Bone marrow mononuclear cells (BMMCs) were obtained from healthy donors (n = 3) and patients with newly diagnosed MM (NDMM, n = 31), and relapsed/refractory MM (RRMM, n = 14) and plasma cell leukemia (PCL, n = 2) who visited the Department of Lymphoma and Myeloma, Institute of Haematology and Blood Disease Hospital, Chinese Academy of Medical Sciences, Peking Union Medical College (Tianjin, China). VRD (Bortezomib [BTZ], lenalidomide, dexamethasone) is the prior treatment status of the refractory patients. The characteristics of the patients with MM and PCL involved in this study were showed on Table 1.

Research involving cell lines

RPMI8226: CVCL_0014, RPMI8226-DOX40, U266: CVCL_0015, OPM2: CVCL_1625, NCI-H929: CVCL_1600, KMS11: CVCL_2989, MM.1R: CVCL_8794 and MM.1s: CVCL_B7F7 were purchased from ATCC. ANBL6: CVCL_5425, and ANBL6-BR: CVCL_QZ43 cells were provided by Dr. Robert Orlowski (MD Anderson Cancer Center, Houston, TX).[28] ARP1: CVCL_D523 and JJN3: CVCL_2078 were gifts from Professor Zhen Cai[29] and Yang Xu (Institute of Haematology, Zhejiang University), respectively. ARD: CVCL_XD83 cell line was kindly provided by Professor Kai Sun (Zhengzhou University People's Hospital). KMS11 drug-resistant cell line (KMS11-BR), which acquired drug resistance by prolonged exposure to a low dose of bortezomib. All the cell lines were subjected to STR profiling and grown under mycoplasma-free conditions at 37 °C and 5% CO_2.

Cell culture and reagents

Primary MM tumour cells and normal plasma cells were isolated from BMMCs by using anti-CD138 microbeads (Miltenyi Biotec). All human MM cell lines were grown in complete culture medium (RPMI 1640 (Gibco, C11875500BT, USA) supplemented with 10% FBS (Gibco, 10,100,147, AUS) and 100 IU/mL penicillin (Gibco, 15,140,122)) in tissue culture flasks at 37 °C in a 5% CO_2 humidified incubator. HEK293T cells were grown in DMEM (Gibco, 11,995,040, USA) basic medium with 10% foetal bovine serum and 100 IU/mL penicillin at 37 °C in a humidified atmosphere containing 5% CO_2. Cell lines were identified prior to use. BTZ (PS-341, Velcade) and Carfilzomib (CFZ) (PR-171) were purchased from Selleck Chemical, Indirubin-3′-monoxime (I3MO, 60807-49-8) and P5091 (882257-11-6) were purchased from MCE.

Cell proliferation assays

Cell proliferation assays were performed using a cell counting kit-8 (CK04, Dojindo Laboratories, Kumamoto, Japan) assay in 96-well plates once daily for 5 days. The absorbance was measured at 450 nm using a SpectraMax 3 microplate reader.

	NDMM (n = 31)	RRMM (n = 14)	PCL (n = 2)
Characteristics			
Median age (years), median (range)	61 (45–81)	54 (36–77)	52 (48–56)
Male, n (%)	18 (58)	8 (57)	2 (100)
Female, n (%)	13 (42)	6 (43)	0 (0)
ISS stage, n (%)			
I	6 (19)	1 (7)	0 (0)
II	13 (42)	5 (36)	0 (0)
III	12 (39)	8 (57)	2 (100)
CAs by iFISH, n (%)			
High-risk[a]	10 (32)	6 (43)	1 (50)
Treatment regimens, n (%)			
VRD	NA	14 (100)	NA

Abbreviations: ISS: international staging system, CAs: cytogenetic abnormalities, iFISH: interphase fluorescence in situ hybridization. VRD (Bortezomib, lenalidomide, dexamethasone). [a]High-risk CA: presence of t (4; 14), t (14; 16) and/or del (17p).

Table 1: **Clinical characteristics of patients with NDMM, RRMM and PCL.**

RT-qPCR assay

Total RNA was extracted using TRIzol (Invitrogen), and cDNA was synthesized by using Hifair III 1st Strand cDNA Synthesis SuperMix (11141-C, Yeasen). RT-qPCR was performed at least thrice using SYBR Green Master Mix (11184ES03, Yeasen, China) on a QuantStudio 5 Real-Time PCR System (Thermo Fisher Scientific). The primers used for RT-qPCR detection were as follows: CRIP1 forward: 5′- GTGTCCCAAGTGCAACAAGG-3′, CRIP1 reverse: 5′-GGTCAGCGTCTTCCCACATT-3'.

Plasmids, shRNAs, and transfection

Flag-CRIP1, empty vector and shRNA plasmids were purchased from Youbio Biological Technology (Changsha, China). The full-length coding sequence of CRIP1 was inserted into pCDH-EF1-MCS-T2A-Puro. shRNAs targeting CRIP1, PSME4 and USP7 were purchased from OBiO Technology (Shanghai, China). Endotoxin-free transfection-grade plasmid DNA was amplified in *E. coli* DH5α Competent Cells (Sangon Biotech, Shanghai, China) and purified with the EndoFree Midi Plasmid Kit (TIANGEN, Beijing, China). Lentiviruses were constructed using psPAX2 and pMD2G and transfected into HEK293T cells with Lipofectamine 3000 (Invitrogen, USA), harvested after 48 or 72 h, and concentrated through ultracentrifugation (20,000×*g*, 2.5 h, 4 °C). The lentivirus was added to 1×10^6 cells along with 8 mg/mL polybrene in a 12-well plate, and stable cells were selected after 72 h using puromycin (60210es25, Yeasen, China) and geneticin (G418; Selleck, USA). The levels of CRIP1 were confirmed using RT-qPCR and western blotting. shRNA sequences are listed as follows: CRIP1-shRNA (5′-AGCACGAAGGCAAACCCTACT-3′); PSME4-shRNA (5′-GCAACTAGTAAATCTCTTTGC-3′); and USP7-shRNA (5′-GTGTCCTATATCCAGTGTAAA-3′).

Western blots

Western blotting was performed as previously described.[10,27] Primary antibodies against CRIP1 (15349-1-AP, RRID: AB_2878128), PA200 (18799-1-AP, RRID: AB_10598020) and USP7 (66514-1-Ig, RRID: AB_2881877) were purchased from Proteintech (Rosemont, IL, USA). Additionally, anti-Ubiquitin (43124, RRID: AB_2799235), anti-DYKDDDDK Tag (14793, RRID: AB_2572291), anti-LC3B (3868, RRID: AB_2137707), anti-GAPDH (#5174, RRID: AB_10622025), anti-β-Actin and secondary antibodies (anti-rabbit (#7074, RRID: AB_2099233) and anti-mouse (#7072, RRID: AB_331144) were purchased from Cell Signaling Technology. The bands were visualized using a ChemiDoc Touch Imaging System (Bio-Rad, Singapore).

Proteasome activity assay

Proteaosome activity assays were conducted using Proteasome-GloTM Chymotrypsin-Like and Caspase-Like Cell-Based Assays (G8660, Promega Corporation, Madison, WI, USA) according to the manufacturer's protocol.

RNA sequencing

RNA sequencing was performed in the ARP1, KMS11 and NCI-H929 cell lines transfected with CRIP1-shRNA/OE or a control vector as described previously.[27] A gene set enrichment analysis (GSEA, V2.2.4, Broad Institute) was performed. The gene expression omnibus (GEO) datasets GSE5900, GSE2658 and GSE31161 were used to investigate the clinical significance of CRIP1. The log-rank test was used to assess the univariate association with disease-related survival in the GSE4581 and GSE136337 datasets. The data are available from the NIH GEO database (GSE248339).

Coimmunoprecipitation (Co-IP)

MM cells (1×10^7) were lysed in native lysis buffer (R0030, Solarbio, Beijing) containing a PI cocktail for 30 min at 4 °C. The cell lysates were incubated with Protein A/G Magbeads (L00277, GenScript) for preclearing. Next, the samples were incubated with 3 μg of antibody overnight followed by incubation with Magbeads at 4 °C for 4 h. Immunoprecipitates were used for immunoblotting with the indicated antibodies or mass spectrometry (MS) to identify the interacting proteins. The following antibodies were used for Co-IP: anti-CRIP1 (ab185558, Abcam), anti-PA200 (18799-1-AP, Proteintech, RRID: AB_10598020), anti-USP7 (66514-1-Ig, Proteintech, RRID: AB_2881877), anti-DYKDDDDK Tag (14,793, Cell Signaling Technology, RRID: AB_2572291) and anti-IgG (3900, Cell Signaling Technology, RRID: AB_1550038).

Autophagosome detection

The pCDH-EF1a-mCherry-EGFP-LC3B plasmid (#170446) used for autophagosome detection was purchased from Addgene (USA). We transfected the lentivirus packaged with the mCherry-GFP-LC3B plasmid into MM cell lines to monitor cell fluorescence by using confocal microscopy.

Myeloma xenograft model

As shown in Fig. 2e, 1×10^6 ARP1 cells with CRIP1 knockdown (CRIP1-shRNA) were injected into the right flank of 6-8-week-old NOD/SCID mice (female) (n = 16, n = 4/group). Depletion of CRIP1 expression was induced with doxycycline (2 mg/mL) as previously described.[27,30] After 7 days, the mice were treated with BTZ (0.5 mg/kg) or PBS twice weekly for 3 weeks. Once the tumour volume reached 2000 mm^3, the mice were euthanized for tumor examination. Tumour volumes were calculated using the following formula: length × $width^2 \times 0.52$.

As shown in Fig. 7e, 5×10^6 per mouse NCI–H929 EV, CRIP1-OE, CRIP1-OE with PSME4-sh, CRIP1-OE with USP7-shRNA and control cells expressing luciferase were injected into the right flank of 7-week-old female NOD/SCID mice (n = 30, n = 3/group) to analyze tumour proliferation. After 7 days, the mice

were treated with BTZ (1 mg/kg) or PBS twice weekly for 3 weeks. The tumour burden was monitored USING bioluminescence imaging once the tumour volume reached 2000 mm^3. Luciferin (75 mg/kg, Sigma–Aldrich, USA) was administered via intraperitoneal (i.p.) injection 10 min before detection using an IVIS Lumina II system (Caliper Life Sciences, Hopkinton, USA).[31] After concluding the treatment, the mice were kept alive for survival analysis. The mice were sacrificed when the tumour volume reached 2000 mm^3.

As shown in Fig. 7h, ARP1 EV and CRIP1-OE cells (1×10^6 cells/mouse) were injected into the left and right flanks of NOD/SCID mice, respectively. Mice were treated with PBS, BTZ (0.5 mg/kg, i.p., twice a week from day 7), P5091 (10 mg/kg, i.p., daily from day 3), I3MO (1.25 mg/kg, i.p., three times a week from day 7) and combination treatment. Tumour volumes were measured using calliper twice a week with a modified ellipsoidal formula: length × $width^2$ × 0.52. Once the tumours reached 2000 mm^3, all mice were sacrificed for harvesting and examination.

All in vivo study procedures were performed according to a protocol, which was approved by the Animal Care and Use Committee (IACUC) of the Institute of Hematology, Chinese Academy of Medical Science.

Statistics

Kaplan–Meier and log-rank tests were used to analyze the differences in survival times between subgroups. Over all (OS) was defined as the time from the start of treatment until death from any cause or until the last date on which the patient was known to be alive. *t* tests were used to compare the two groups. Kolmogorov–Smirnov test was used to investigate the clinical significance of CRIP1 in GEO datasets: GSE2658, GSE31161 and GSE5900. Analyses were performed using SPSS version 25.0 and GraphPad Prism (version 8.01, GraphPad Software Inc.). P values less than 0.05 were considered to indicate statistically significant differences. *P < 0.05; **P < 0.01; ***P < 0.001.

Role of founders

The founders played no roles in the study design, data collection, data analysis, interpretation, or the writing of the manuscript.

Study approval

This study was conducted in accordance with the guidelines of the Declaration of Helsinki and approved by the local institutional Ethics Committee (protocol code KT2020010-EC-2). Informed consent was obtained from all subjects involved in the study. All the in vivo procedures in vivo were performed according to a protocol approved by the Animal Care and Use Committee (IACUC) of the Institute of Haematology, Chinese Academy of Medical Science. All the mouse experiments were approved (the reference number is IHCAMS DWLL-2018-KT007-1) by the IACUC of the Institute of Haematology, Chinese Academy of Medical Science.

Results

High-level CRIP1 is associated with poor outcome in patients with MM

Based on publicly available GEO datasets (GSE2658, GSE31161 and GSE5900) of patients with MM, we found that the expression of CRIP1 is heterogeneous in these patients. The levels of CRIP1 were significantly increased in patients with NDMM (n = 1339) compared to healthy donors (n = 22), (P < 0.01, Kolmogorov–Smirnov test). Notably, the level of CRIP1 was higher in patients with RRMM (n = 255) than those in NDMM (n = 1339) (P < 0.01, Kolmogorov–Smirnov test) (Fig. 1a). Kaplan–Meier analysis of the public MM datasets GSE2658 and GSE4581 showed that patients with MM with high levels of CRIP1 had inferior outcomes (Fig. 1b, P < 0.001, *t* test). Even among patients treated with BTZ, the OS of patients with high CRIP1 levels was significantly shorter than that of patients with low CRIP1 level (Fig. 1c, P < 0.0001, *t* test). Zhan F et al. validated seven disease subtypes named the UAMS 7 subgroups that were strongly influenced by known genetic lesions, including c-MAF- and MAFB-, CCND1- and CCND3-, and MMSET-activating translocations and hyper diploidy.[32] Here, we used the GSE2658 dataset to investigate the CRIP1 levels in these seven disease subtypes of patients with MM. Our results showed that CRIP1 was significantly increased in the MAF and PR (proliferation) groups, which were identified as the high-risk subgroups for MM by Zhan's study (P < 0.0001, *t* test, Fig. 1d). High MAF expression is related to the t[14,16] translocation. Western blotting analysis showed CRIP1 protein levels were relative higher in MM cell line with t,[14,16] as Fig. 1e showed. This result suggests that cytogenetic abnormality involves in the regulation of CRIP1 expression in MM cells, which causes the heterogeneously increase of CRIP1 in a subset of MM cells and associated with inferior outcome. In addition, we found that CRIP1 levels was increased in drug-resistant MM cell lines (KMS11/BR, ANBL-6/BR, MM.1R and RPMI-8226/Dox40) compared to that in the parental cell lines (Fig. 1e). The transcriptome dataset of the Encyclopedia of Cancer Cell Lines further confirmed that the level of CRIP1 was significantly higher in MM cell lines than those with other haematological malignancies (Fig. 1f). Western blotting assays were also utilized to detect the protein level of CRIP1 in purified $CD138^+$ cells from patients with NDMM(n = 20), patients with RRMM(n = 14) and patients with plasma cell leukaemia (PCL) (n = 2) and with normal plasma cells (n = 3) as controls. The results showed that the level of CRIP1 in $CD138^+$ MM cells was significantly higher than that in normal plasma cells,

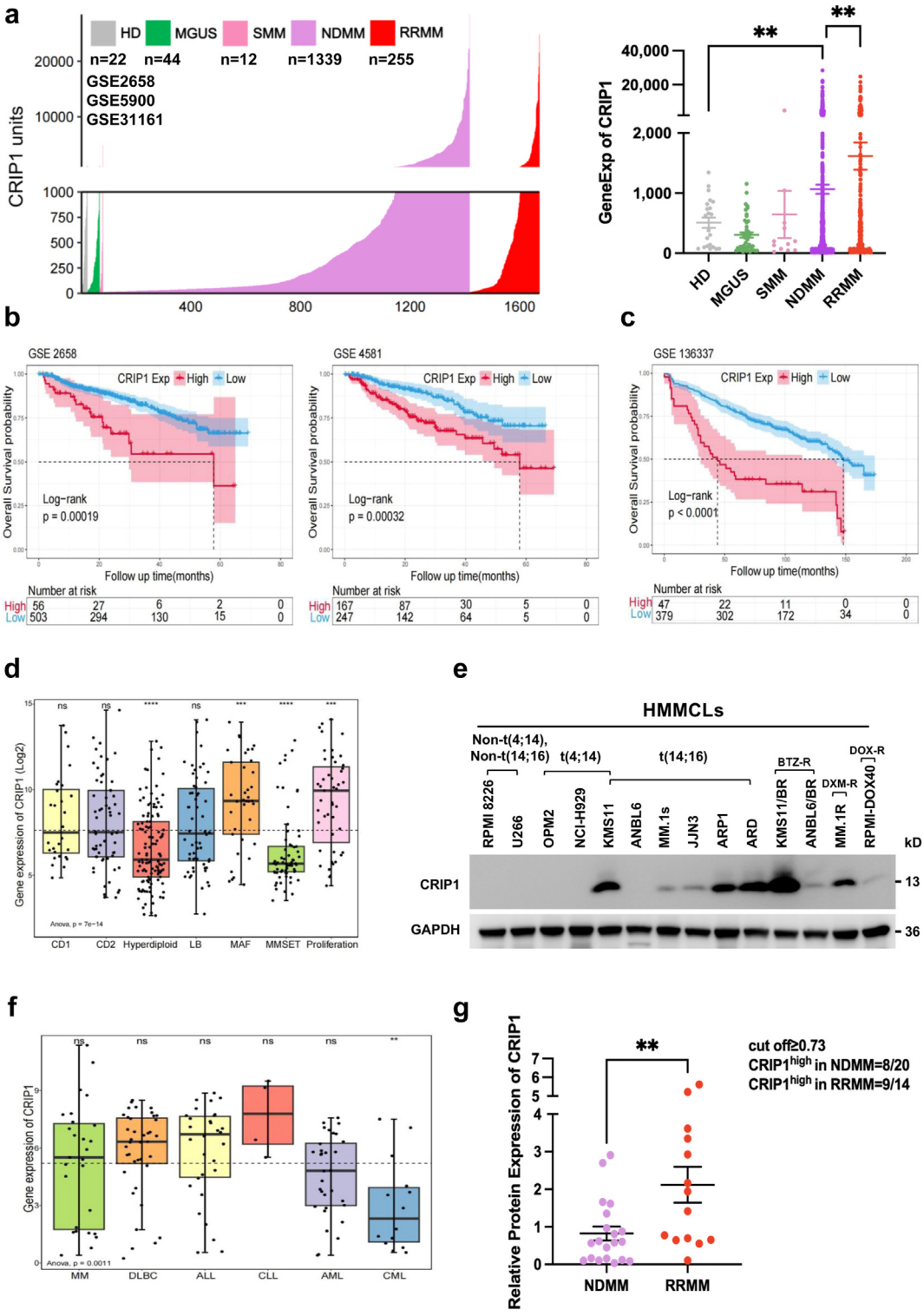

Fig. 1: **High-level CRIP1 links poor prognosis in Patients with MM** (a). The clinical significance of CRIP1 in the GEO Series of patients with MM was investigated. The expression of CRIP1 was compared in plasma cells from healthy donors (HD, n = 22), individuals with monoclonal gammopathy of undetermined significance (MGUS, n = 44), individuals with smouldering multiple myeloma (SMM, n = 12), patients with newly diagnosed MM (NDMM, n = 1339) and relapsed/refractory multiple myeloma (RRMM, n = 255) from the GEO Series (GSE2658, GSE31161

and the level of CRIP1 in patients with RRMM was even higher than that in patients with NDMM. The relative CRIP1 protein levels were analyzed in all patients with MM (Fig. 1g and Supplementary Fig. S1). Together, the results indicated that the level of CRIP1 is the heterogeneously increased in a subset of MM cells, especially in high-risk patients, and that the level of CRIP1 serves as a poor prognostic biomarker for MM.

CRIP1 promotes aggressive growth and drug-resistance in MM

To explore the role of CRIP1 in MM pathogenesis, we constructed CRIP1 overexpression (CRIP1-OE) and CRIP1 knockdown (CRIP1-shRNA) cell lines. A doxycycline-inducible CRIP1-shRNA vector was transduced into the ARP1 and KMS11 (high CRIP1 expression) myeloma cell lines, and a CRIP1-OE vector was transduced into the ARP1 and NCI-H929 (low CRIP1 expression) cell lines. An in vitro study showed that CRIP1 knockdown repressed the proliferation of MM cells after day 4 compared to the control, and the overexpression of CRIP1 significantly promoted cell proliferation after day 4 compared to the control as shown in Fig. 2a. Furthermore, the results of the Transwell assay indicated that CRIP1 knockdown suppressed the migration of MM cells to the lower chamber through the Matrigel-coated membrane ($P < 0.01$, *t* test). Conversely, CRIP1-OE promoted MM cells (ARP1 and NCI-H929) invasion and migration compared to the empty vector (EV) control group ($P < 0.01$, *t* test, Fig. 2b and Supplementary Fig. S2a). Flow cytometry analysis showed that CRIP1 accelerated cell cycle progression by regulating the S-Phase ($P < 0.05$, *t* test; Fig. 2c), which could explain for the aggressive growth of CRIP1 overexpression cells.

Based on the data shown above (Fig. 1) that CRIP1 was highly expressed in patients with MM, especially in patients with RRMM, and correlated with their inferior outcomes, we speculated that CRIP1 overexpression is involved in the drug resistance of MM. To test this hypothesis, we evaluated the effect of CRIP1 on the drug sensitivity of MM cells. Cell viability and IC50 analyses showed that the sensitivity of MM cells to the PIs, including BTZ (Fig. 2d) and CFZ (Supplementary Fig. S2b) was decreased in CRIP1-OE cells but increased in CRIP1 knockdown cells. These results indicated that CRIP1 knockdown increased PIs sensitivity. To further analyze the correlation between CRIP1 expression and PIs resistance, we knocked down CRIP1 in KMS11-BTZ resistant cell line. We found that CRIP1 knockdown was correlated with reversed BTZ sensitivity. Knockdown CRIP1 level in KMS11-BR cells, the sensitivity to BTZ treatment was rescued (Fig. 2d). Given the distinct endogenous levels of CRIP1 in KMS11 and NCI-H929 cell (shown in Fig. 1e), we compared the drug sensitivity in these MM cell lines. We found that KMS11-Scr (IC50 = 15.37 nM) are more resistance to bortezomib treatment than NCI-H929-EV cells (IC50 = 6.23 nM). Then, we correlated CRIP1 protein level and PIs sensitivity in a large panel of MM cell lines. IC50 values were calculated and compared with CRIP1 gene expression across all cell lines (Supplementary Fig. S2c). The results indicated that endogenous CRIP1 expression was also associated with PIs sensitivity ($P < 0.05$, $n = 14$, Pearson correlation coefficients). We used a myeloma xenograft mouse model to confirm the effects of CRIP1 on MM cell proliferation, drug resistance and disease progression. A murine subcutaneous transplantation model of ARP1 with CRIP1 inducible knockdown cells was used. Monitoring of tumour volume and weight showed that CRIP1 knockdown significantly suppressed MM cell proliferation in vivo ($P < 0.01$, *t* test). Under treatment with BTZ, the growth inhibition of MM cells was significantly higher in the CRIP1 knockdown group than in the scramble group ($P < 0.05$, *t* test (Fig. 2e and f and Supplementary Fig. S2d). Overall, these findings indicated that high levels of CRIP1 promote aggressive proliferation of MM cells and induce PIs resistance.

CRIP1 induces drug resistance via dual-regulation proteasome and autophagy activity

Next, we explored the mechanisms by which CRIP1 decreased PIs sensitivity in MM cells. First, RNA sequencing and bioinformatics analyses were performed on CRIP1 knockdown cells. Notably, Gene ontology (GO) biological process analysis indicated that the proteasome-mediated ubiquitin-dependent degradation and that autophagy pathways were significantly enriched in CRIP1 knockdown cells (Fig. 3a and b). MM cells with lower proteasome activity and higher proteasome load may be more sensitive to PIs treatment.[33,34]

and GSE5900). (left figure, $P < 0.05$, Kruskal–Wallis test; right figure, $P < 0.01$, Kolmogorov–Smirnov test). (b). Kaplan–Meier analysis was performed in patients with MM with high or low CRIP1 expression enrolled in GSE2658 ($P < 0.001$, log-rank test) and GSE4581 ($P < 0.001$, log-rank test). (c). Kaplan–Meier analysis was performed in patients with MM with BTZ treatment enrolled in GSE136337 ($P < 0.0001$, log-rank test). (d). GSE2658 was applied to investigate the CRIP1 level of patients with MM in UAMS 7 subgroups reported by Zhan ($P < 0.0001$, ordinary one-way ANOVA). (e). The CRIP1 protein expression levels in HMMCLs were detected by Western blotting. (f). The gene expression levels of CRIP1 were analysed in various haematological malignancies in the CCLE database ($P < 0.01$, ordinary one-way ANOVA). (g). The expression of CRIP1 in bone marrow plasma cells of NDMM ($n = 20$) and RRMM ($n = 14$) was assessed via western blotting (refer to Supplementary Fig. S1) and represented as scatter plots ($P < 0.01$, unpaired t test). The statistical significance for the above data is indicated as follows: * indicates $P < 0.05$; ** indicates $P < 0.01$; *** indicates $P < 0.001$.

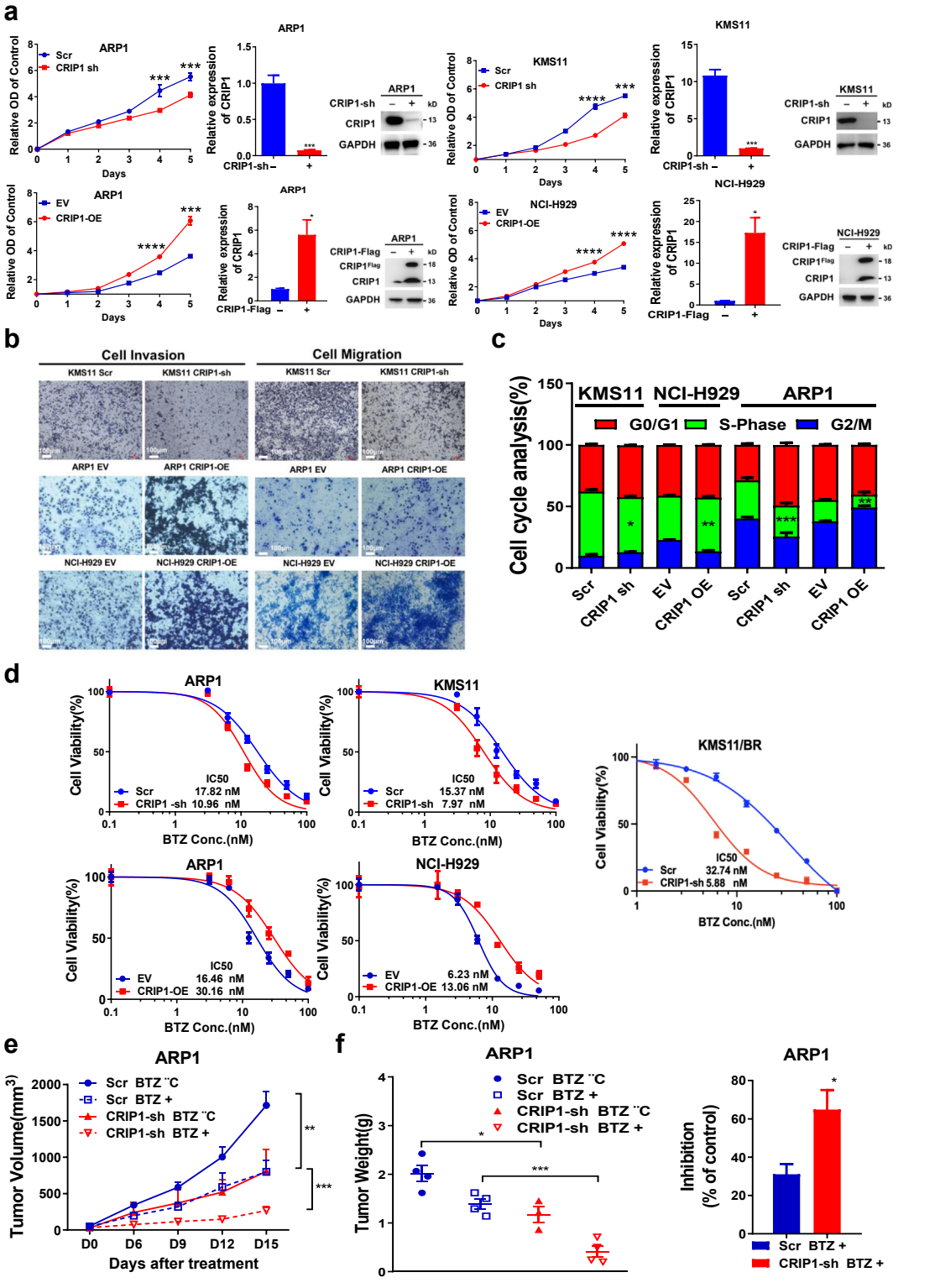

Fig. 2: **CRIP1 promotes tumour cell growth and induces drug-resistance** (a). The efficiencies of CRIP1 knockdown in the ARP1 and KMS11 cell lines and CRIP1 overexpression in the ARP1 and NCI-H929 cell lines were examined by using qPCR and Western blotting. The proliferation of cells was monitored daily with a CCK-8 assay for 5 days. (b). The effect of CRIP1 expression on the invasion and migration capabilities of

Therefore, we speculated that CRIP1 playes a critical role in the regulation of proteasomal activity and protein load in MM cells, which induces drug resistance in MM. As expected, we found that the caspase-like (C-L), chymotrypsin-like (CT-L) and trypsin-like (T-L) peptidase activities of the proteasome were significantly reduced in CRIP1 knockdown MM cell lines and elevated in CRIP1-OE cells (Fig. 3c). More ubiquitinated proteins accumulated in CRIP1 knockdown cells, and fewer ubiquitinated proteins accumulated in CRIP1-OE cells (Fig. 3d). Therefore, damage to proteasome activity induced by CRIP1 knockdown causes proteasomal stress, leading to the accumulation of ubiquitinated proteins in cells.

Autophagy is a catabolic process in which intracellular components are degraded and recycled by the lysosomes and autophagosomes.[35] Accumulating evidence indicates that increased autophagy contributes to drug resistance and that autophagy inhibition is an effective strategy to overcome drug resistance and improve antitumor therapy.[36–38] Transformation of LC3B-I to LC3B-II is a widely accepted as a biomarker of autophagy.[39] As shown in Fig. 3e, the level of LC3B II was decreased in MM cells following the knocking down of CRIP1. CRIP1-OE cells showed increased LC3B-II levels in both ARP1 and NCI-H929 MM cell lines. Furthermore, variations in LC3B-II and LC3B-I levels after treatment with chloroquine (CQ), a specific inhibitor of autophagy, showed that the degradation of LC3B-II was significantly inhibited in KMS11 and NCI-H929 MM cell lines, and the LC3B-II/LC3B-I ratio significantly increased. The LC3B-II/LC3B-I ratio was significantly decreased in CRIP1 knockdown MM cells after CQ treatment compared to control cells (Fig. 3f & Supplementary Fig. S3a). These findings suggested that high levels of CRIP1 efficiently promoted autophagy in MM cells. A tracking system for autophagy dynamics was used to further confirm the effects of CRIP1 on autophagy induction. The lentivirus packaged plasmid mCherry-GFP-LC3B was transfected into the KMS11 CRIP1 knocking down and NCI-H929 CRIP1-OE MM cell lines. Autophagosomes were labelled with yellow, and autolysosomes were labelled with red because of GFP fluorescence quenching in an acidic lysosomal environment. The confocal puncta of LC3B level in each group were also quantified. An increased fraction of autophagosomes was observed in CRIP1-OE cells (NCI-H929) compared to that in EV control cells after CQ treatment (Fig. 3g & Supplementary Fig. S3b). In contrast, the CRIP1 knockdown decreased autophagosome maturation. These results indicated that CRIP1 promotes autophagosome maturation in MM cells. Next, we explored the rescue of PIs resistance induced by CRIP1 overexpression via the inhibition of autophagy activity. MM cells with CRIP1-knockdown or CRIP1-OE were treated with BTZ/CFZ and CQ alone or in combination. Consistent with previous data, CRIP1 knockdown increased the sensitivity to PIs treatment, whereas CRIP1-OE induced the PIs resistance. Notably, compared with the single agent treatment, combination treatment with PIs and CQ significantly suppressed the cell viability of MM cells (Fig. 3h). These findings suggest that CRIP1 plays a substantial role in regulating the drug response to PIs by duel modulating proteasome and autophagy activitives in MM cells. Hence, targeting CRIP1 would rescue the drug-resistance.

CRIP1 regulates the stability of PA200

Next, we explored the mechanisms through which CRIP1 promotes proteasome activity and autophagy. PA200 is an activator subunit of the proteasome. Our previous study reported that PA200 levels were elevated in patients with MM and positively correlated with proteasome activity.[40] PA200 also affects aggresomal and autophagy formation.[41] Therefore, we hypothesized that CRIP1 upregulates proteasome activity and autophagy by regulating PA200 expression. Co-IP analysis showed that CRIP1 bound to PA200 in both the ARP1 and KMS11 MM cell lines (Fig. 4a). Interestingly, we noted that the protein level of PA200 positively correlated with CRIP1 levels in the NCI-H929 and ARP1 cell lines, as shown in Fig. 4b. To further identify whether CRIP1 regulates the proteasome activity and autophagy through PA200, we knocked down PSME4 (gene for PA200) expression in CRIP1-OE ARP1 and NCI-H929 cell lines, and found that PA200 protein levels varied with PSME4 knockdown, in addition to transcription levels (Fig. 4c). Next, the proteasome and autophagy activities were examined. Consistent with the previous data, PSME4 knockdown significantly decreased the proteasome activity (Fig. 4d) and suppressed autophagy by decreasing LC3B-II levels (Fig. 4e) in CRIP1-OE MM cell lines. These results demonstrated that CRIP1 enhances

myeloma cells was observed using a Transwell assay. Scale bar = 100 μm. (c). The cell cycle was analysed in MM cell lines by flow cytometry and presented as a bar chart with three replicates for each group. (d). The sensitivity of multiple myeloma cells with CRIP1 knockdown or overexpression to bortezomib treatment was assessed. (e). A total of 1×10^6 ARP1 cells with CRIP1 knockdown (CRIP1-shRNA) were injected into the right flank of 6- to 8-week-old NOD/SCID mice (n = 16, n = 4/group). These mice were subsequently treated with either PBS or bortezomib (0.5 mg/kg). Depletion of CRIP1 expression was induced using doxycycline (2 mg/mL). Tumour volumes were measured twice a week and are depicted in a line graph. Tumours were harvested before reaching a volume of 2000 mm^3. (f). Tumour weight was measured, and the bortezomib inhibition rate on the tumours was calculated. The above data statistical analysis employed t-test, with the significance levels denoted as follows: * for $P < 0.05$, ** for $P < 0.01$, and *** for $P < 0.001$.

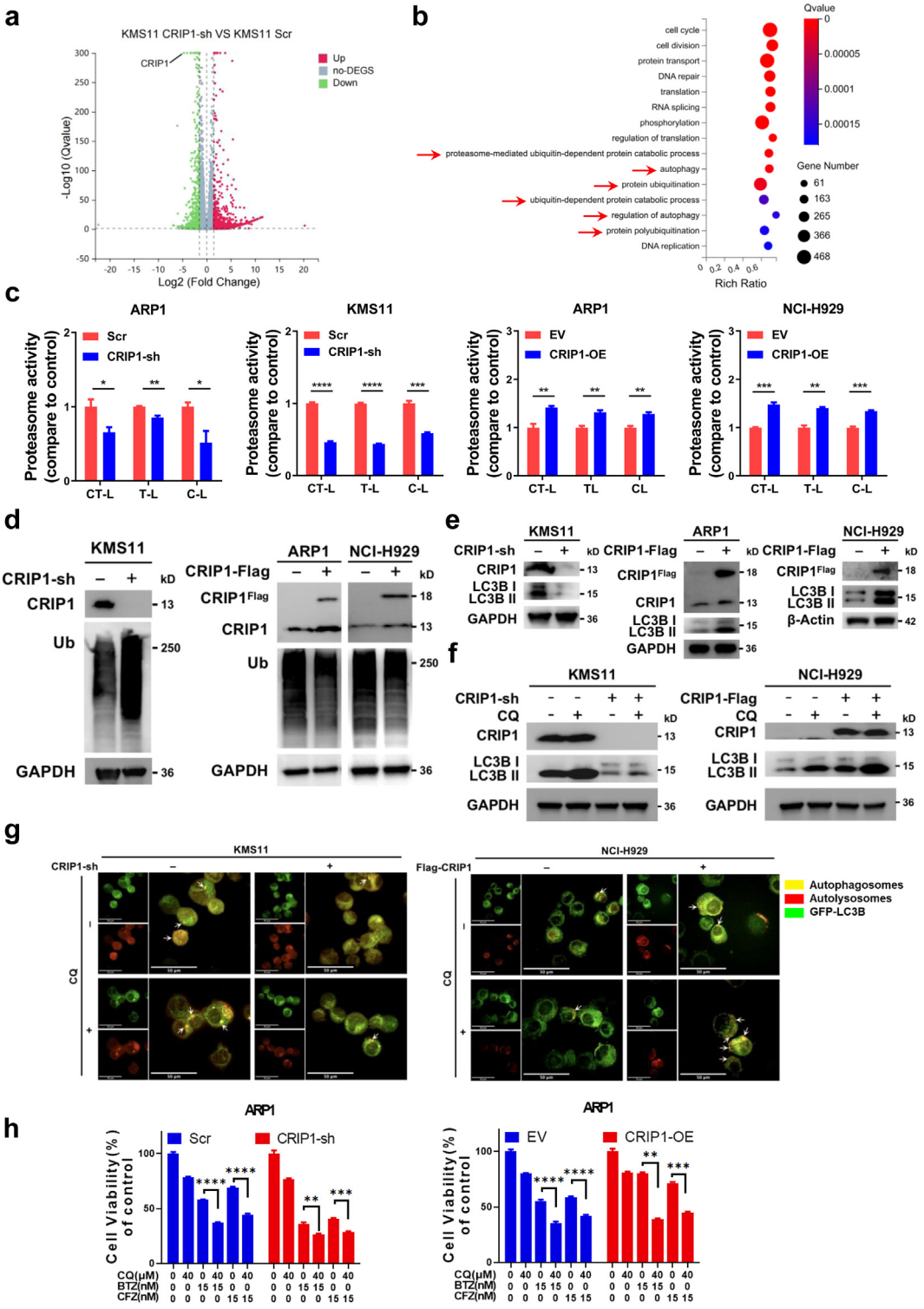

***Fig. 3:* CRIP1 dual-regulates proteasome activity and autophagy** (a). RNA sequencing was performed in the KMS11 Scr and CRIP1-sh cell lines. The differentially expressed genes (DEGs) (|log (FC)| ≥ 1.5) between the two groups are shown with a volcano plot. (b).GO biological process analysis was performed in DEGs of KMS11 Scr and CRIP1-sh cells. (c).The chymotrypsin-like (CT-L), trypsin-like (T-L) and caspase-like (C-L) activities of the 20S proteasome were analysed in CRIP1 knockdown or overexpression MM cell lines. (d). Western blotting was employed to analyse the impact of CRIP1 knockdown and overexpression on the ubiquitination of myeloma cells. (e). Western blotting was utilized to

proteasome activity and autophagy by binding to and regulating PA200 levels in MM.

CRIP1 was the substrate of USP7

Tandem affinity purification/MS analysis was performed to investigate how CRIP1 stabilizes PA200 and to better understand the signaling pathways involved in CRIP1-mediated PIs resistance. CRIP1 was immunoprecipitated using anti-FLAG antibodies in RPMI 8226 and MM.1s CRIP1-OE cells (with 3 × FLAG). The results showed that 1528 proteins were identified as binding with CRIP1. GO annotation analysis indicated that the proteins bound to CRIP1 were enriched in proteolysis, ubiquitin-dependent protein catabolic process and proteasome core complex (Fig. 5a and Supplementary Table S1), strongly suggesting that CRIP1 is critical for the regulation of proteostasis via multiple signaling pathways in MM. Among these proteins, we were particularly interested in ubiquitin-specific protease 7 (USP7), also known as HAUSP, which is a deubiquitinating (DUB) enzyme that stabilizes substrate proteins. Our previous study showed that USP7 was overexpressed in MM cells and plays a critical role in protein stabilization and drug-resistance in MM.[10,42] Therefore, we preformed Co-IP and western blotting to further confirm the binding between CRIP1 and USP7 in RPMI 8226 and MM.1s cells expressing CRIP1-OE (3 × FLAG). These results confirmed the binding between USP7 and CRIP1 in MM cell lines (Fig. 5b). Next, we explored the effects and the mechanisms of USP7 binding to CRIP1. We observed that the level of CRIP1 was obviously downregulated if the USP7 activity was repressed by the treatment with P5091 (a USP7 inhibitor) in both wild-type and CRIP1-OE MM cells in a dose-dependent manner. Elevated CRIP ubiquitination was observed in RPMI 8226 CRIP1-OE (3 × FLAG) cells after blocking deubiquitination with P5091 treatment (Fig. 5c). To further confirm the regulatory mechanism of USP7 on CRIP1, we knocked down the USP7 expression using shRNA in ARP1 CRIP1-OE cells and examined the effect of USP7 knockdown on CRIP1 ubiquitination. Consistent with the results of P5091 treatment, CRIP1 ubiquitination was elevated with USP7 knockdown (Fig. 5d). Moreover, the P5091 inhibition effect on CRIP1 was reversed through MG132 administration, which blocked proteasome activity (Fig. 5e). Taken together, our data suggest that CRIP1 is a substrate of USP7 and the degradation of CRIP1 was dependent on the UPS. Because of the elevated level of USP7 in MM cells,[43] we speculated that high levels of USP7 promote the stabilization and accumulation of CRIP1 in MM cells. Our study further confirmed our hypothesis using a panel of MM cell lines and primary patient samples. The results indicated that CRIP1 expression correlated with USP7 in patient samples ($R = 0.8694$, $P < 0.01$, $n = 10$) and MM cell lines ($R = 0.4059$, $P < 0.05$, $n = 14$), Pearson correlation coefficients) (Fig. 5f and Supplementary Fig. S4).

CRIP1 facilitates the interaction between PA200 and USP7

Based on the above findings, we investigated the interactions and biological functions of CRIP1, USP7 and PA200. We measured the levels of CRIP1 and PA200 in MM cells by blocking USP7 with specific inhibitor P5091. Interesting, blocking USP7 obviously decreased the levels of PA200 in ARP1 and NCI-H929 wild-type MM cell lines (Fig. 6a) in a dose-dependent manner (Fig. 6b). The levels of both CRIP1 and PA200 decreased when USP7 was knocked down in CRIP1-OE cells (Fig. 6c). These results suggest that blocking USP7 activity triggers the downregulation of CRIP1 and PA200. CRIP facilitates the binding of PA200 to USP7 to stabilize the protein of PA200. Co-IP analysis confirmed an endogenous interaction between CRIP1, USP7 and PA200 in wild-type MM cells. CRIP1, USP7, and PA200 combine to form a complex (Fig. 6d). The LIM domains of CRIP1 mediate specific protein–protein interactions. We speculated that CRIP1 was necessary for the interaction between USP7 and PA200. To test this hypothesis, we examined the impact of CRIP1 on USP7 and PA200 binding in CRIP1 knockdown and overexpression cell lines. As expected, CRIP1 knockdown substantially suppressed the binding between USP7 and PA200, but increased the ubiquitination of PA200 in CRIP1 knockdown MM cells (Fig. 6e). In contrast, CRIP1 overexpression enhanced the interaction between USP7 and PA200, and decreased the ubiquitination of PA200 (Fig. 6f). To further clarify whether CRIP1 promotes the stabilization of PA200 mediated by USP7 via the formation of the CRIP1/USP7/PA200 complex, half-life experiments were performed using cycloheximide to inhibit the synthesis of new proteins. Our results clearly indicate that high levels of CRIP1 suppress the degradation of PA200 and enhanced its stability of PA200 in MM cell lines (Fig. 6g).

examine the cellular autophagy levels associated with differential CRIP1 expression. (f). After treatment of MM cells with chloroquine (10 μM, 24 h), the accumulation of LC3B-II protein was analysed using western blotting. (g). The MM cells were treated with chloroquine (CQ) (10 μM 24 h) to inhibit lysosomal degradation. The expression of mCherry-EGFP-LC3B was visualized in CRIP1 knockdown or CRIP1-overexpressing MM cells using a spinning disk confocal microscope with 488-nm and 561-nm lasers. Scale bar = 50 μm. The confocal puncta of LC3B level in each group were also quantified (shown in Supplementary Fig. S3b). (h). Cell viability was determined by the CCK-8 assay following single or combined treatments with CQ (40 μM) and BTZ/CFZ (15 nM) for 24 h in ARP1 CRIP1 overexpression/knockdown cells. The above data statistical analysis employed t-test, with the significance levels denoted as follows: * for $P < 0.05$, ** for $P < 0.01$, *** for $P < 0.001$, and **** for $P < 0.0001$.

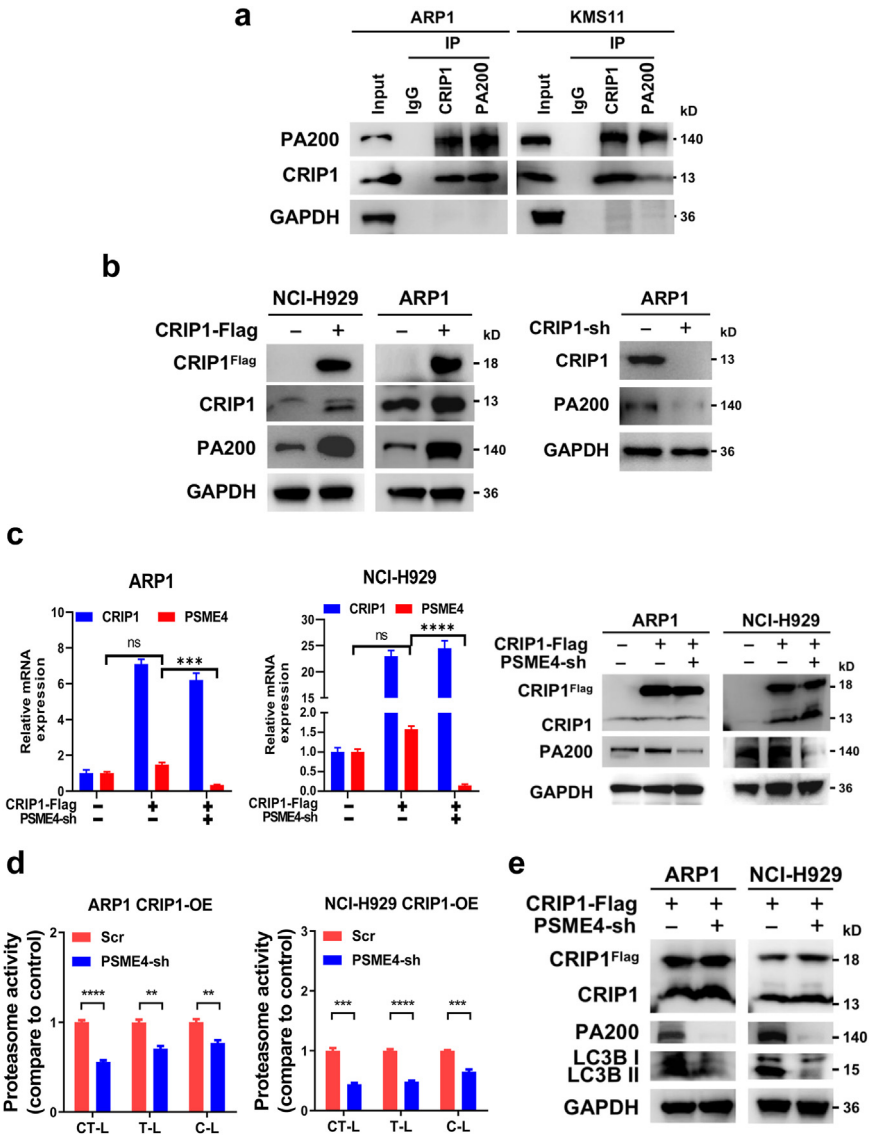

Fig. 4: **CRIP1 stabilizes PA200** (a). Nondenatured lysis of ARP1 and KMS11 cells was performed, followed by immunoprecipitation using IgG, CRIP1 and PA200 antibodies. Western blotting was carried out with PA200 and CRIP1 antibodies. (b).The protein levels of CRIP1 and PA200 were analysed in NCI–H929 CRIP1 OE and ARP1 CRIP1 sh cells through Western blotting. (c).PSME4-shRNA was transfected into ARP1 CRIP1-OE and NCI–H929 CRIP1-OE cells, and the expression levels of CRIP1 and PA200 were analysed via RQ-PCR and Western blotting. (d).Proteasome activities were assessed in CRIP1-overexpressing cells upon knockdown of PSME4, with the experiment repeated three times. (e).Western blotting was carried out to analyse the impact of PSME4 knockdown on cellular autophagy in ARP1 and NCI–H929 CRIP1-overexpressing cell lines. The above data statistical analysis employed t-test, with the significance levels denoted as follows: * for $P < 0.05$, ** for $P < 0.01$, *** for $P < 0.001$, and **** for $P < 0.0001$.

In summary, our study strongly supports that CRIP1 is necessary for the USP7-PA200, which stabilizes PA200 mediated by USP7.

Blocking USP7 or PA200 reduces CRIP1-induced drug-resistance

CRIP1 overexpression reduced the sensitivity of MM cells to BTZ, as previously shown (Fig. 2d), and blocking the activity of USP7 with P5091 depleted the protein levels of CRIP1 (Fig. 5d). Next, we explored whether USP7 involves CRIP1-induced BTZ drug resistance in MM cells using in vitro and in vivo studies. As shown in Fig. 7a, CRIP1 overexpression decreased the sensitivity of MM cells to BTZ-induced apoptosis. The combination of P5091 and BTZ efficiently decreased the cell viability. These results demonstrated that USP7

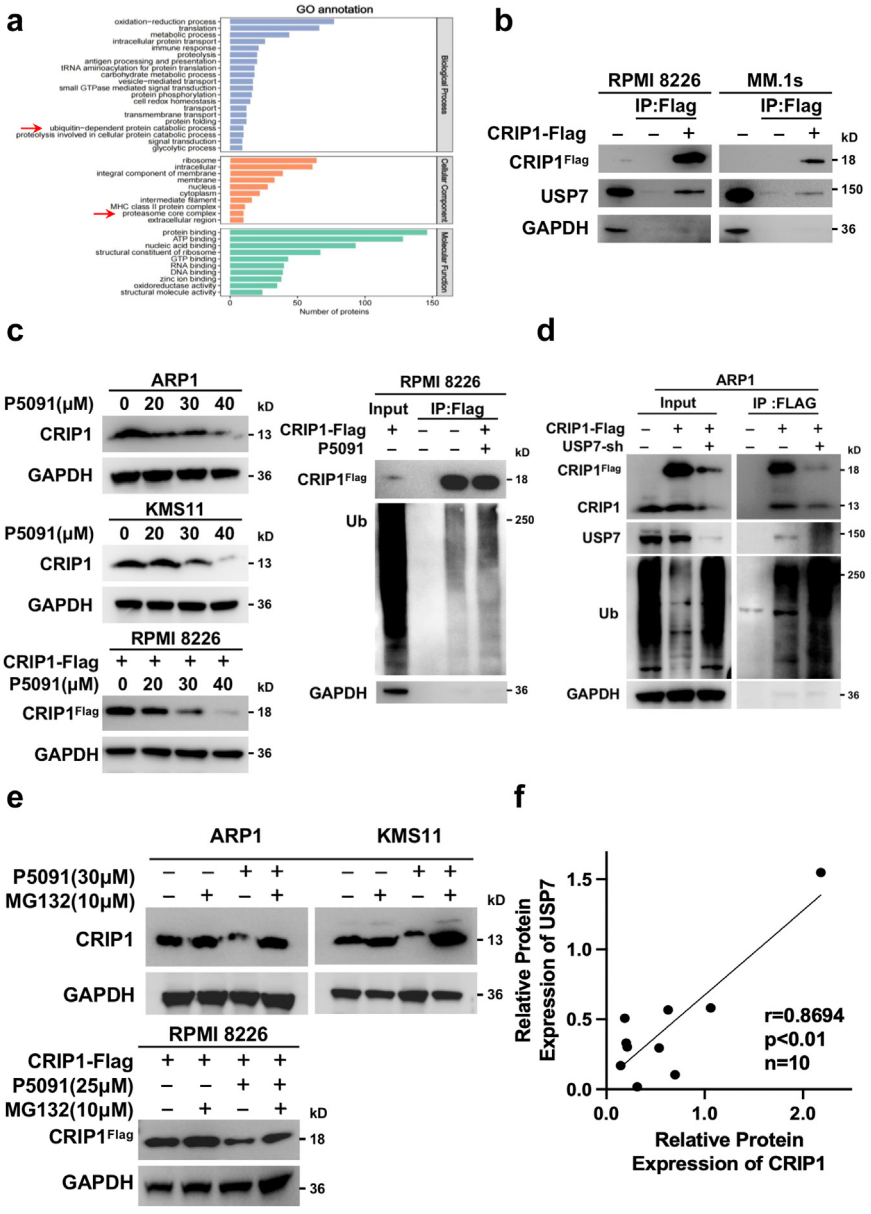

***Fig. 5:* CRIP1 was a substrate of USP7** (a). CRIP1 protein was immunoprecipitated from RPMI 8226 cells, and the proteins interacting with CRIP1 were analysed with immunoprecipitation-mass spectrometry. GO enrichment analysis was performed to analyse the signalling pathway interacting with CRIP1. (b). RPMI 8226 CRIP1-OE and MM.1s CRIP1-OE cells were subjected to immunoprecipitation using anti-Flag affinity purification gel, and the interaction between USP7 and CRIP1 protein was examined using Western blot analysis. (c). ARP1, KMS11 and 8226 CRIP1-OE cells were treated with P5091 (0, 20, 30 and 40 μM for 12 h), and CRIP1 protein was assessed by Western blotting. RPMI 8226 CRIP1-OE cells were treated with or without P5091 (10 μM, 12 h). Subsequently, immunoprecipitation was performed using an anti-Flag affinity purification gel, and the CRIP1 and ubiquitinated proteins was detected through Western blotting. RPMI 8226 EV cells were utilized as a control. (d). After knockdown of USP7 in ARP1 CRIP1 OE cells, Flag antibody was utilized for co-immunoprecipitation followed by western blotting to detect changes in CRIP1 ubiquitination. (e). ARP1, KMS11, and 8226 CRIP1-OE cells were treated with P5091 (25, 30 μM) or MG132 (10 μM) alone or in combination, and the CRIP1 protein was assessed using Western blotting. (f). The protein levels of CRIP1 and USP7 in bone marrow plasma cells of NDMM, RRMM and PCL (n = 10) were determined through Western blotting (shown in Supplemental Fig. S1), followed by correlation analysis of these two proteins using the Pearson coefficient.

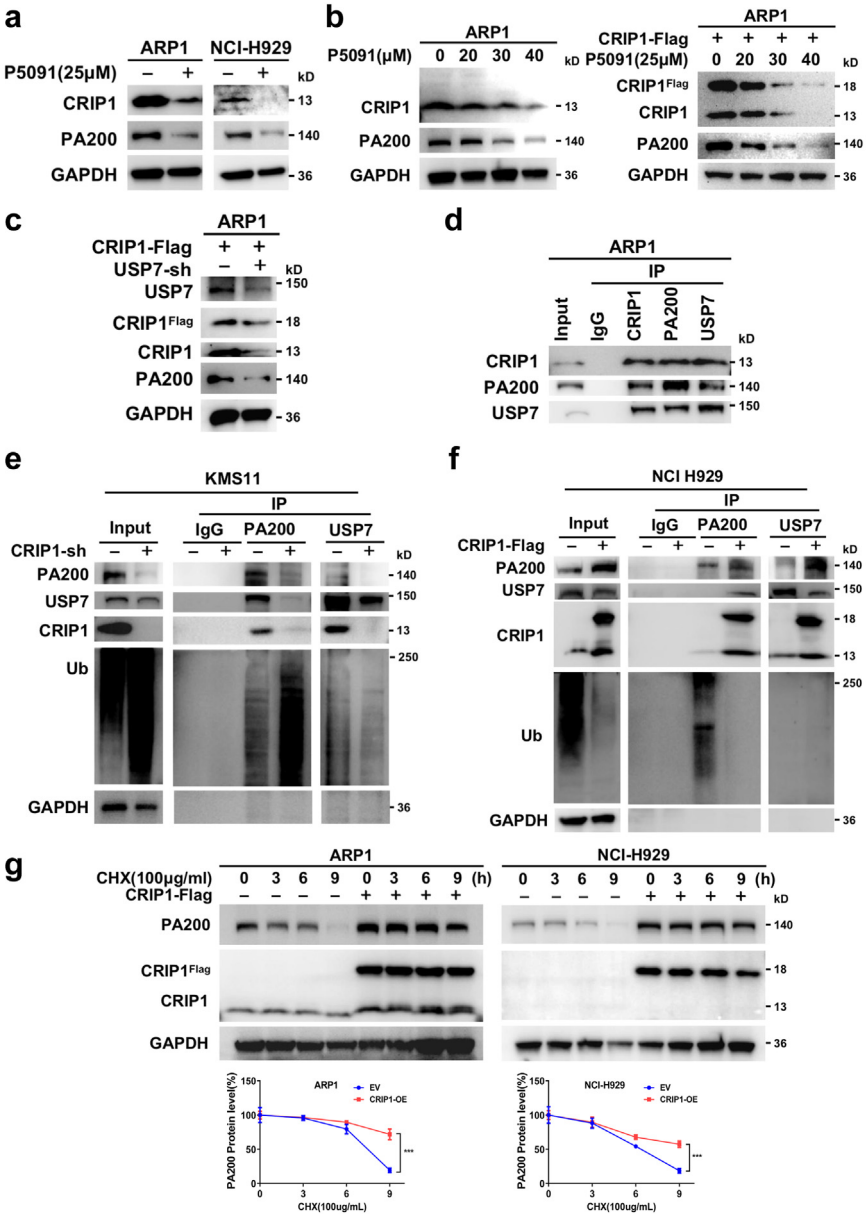

Fig. 6: **CRIP1 forms a complex with USP7/PA200 and facilitates PA200 stabilization** (a). The effects of P5091 treatment (25 μM, 12 h) on the protein levels of CRIP1 and PA200 were assessed in ARP1 and NCI-H929 cells via Western blot analysis. (b). The effects of increasing concentrations (0, 20, 30, and 40 μM) of P5091 treatment on CRIP1 and PA200 expression were analysed via Western blot analysis in ARP1 and ARP1 CRIP1-OE cells. (c). After transfection of USP7-shRNA into ARP1 CRIP1-OE cells, the protein levels of USP7, CRIP1 and PA200 were analysed using Western blot analysis. (d).Nondenaturing lysis of ARP1 cells was performed, followed by immunoprecipitation using CRIP1, PA200, and USP7 antibodies to detect protein–protein interactions. (e and f). Protein–protein interactions were determined via immunoprecipitation using PA200 or USP7 antibodies, followed by Western blot analysis of USP7, PA200, CRIP1, and ubiquitin (Ub) proteins in KMS11 CRIP1-shRNA (e) and NCI-H929 CRIP1-OE (f) cells. (g). ARP1 EV, ARP1 CRIP1-OE, NCI-H929 EV, and NCI-H929 CRIP1-OE cells were treated with 100 μg/mL cycloheximide (CHX) for 0, 3, 6, and 9 h, respectively. The protein levels of PA200 and CRIP1 were analysed by Western blot analysis. The protein bands were qualified by using Image J software. The protein level of PA200 relative to GAPDH was calculated, and a line graph was generated to assess the degradation rate of PA200 ($P < 0.001$, unpaired t test).

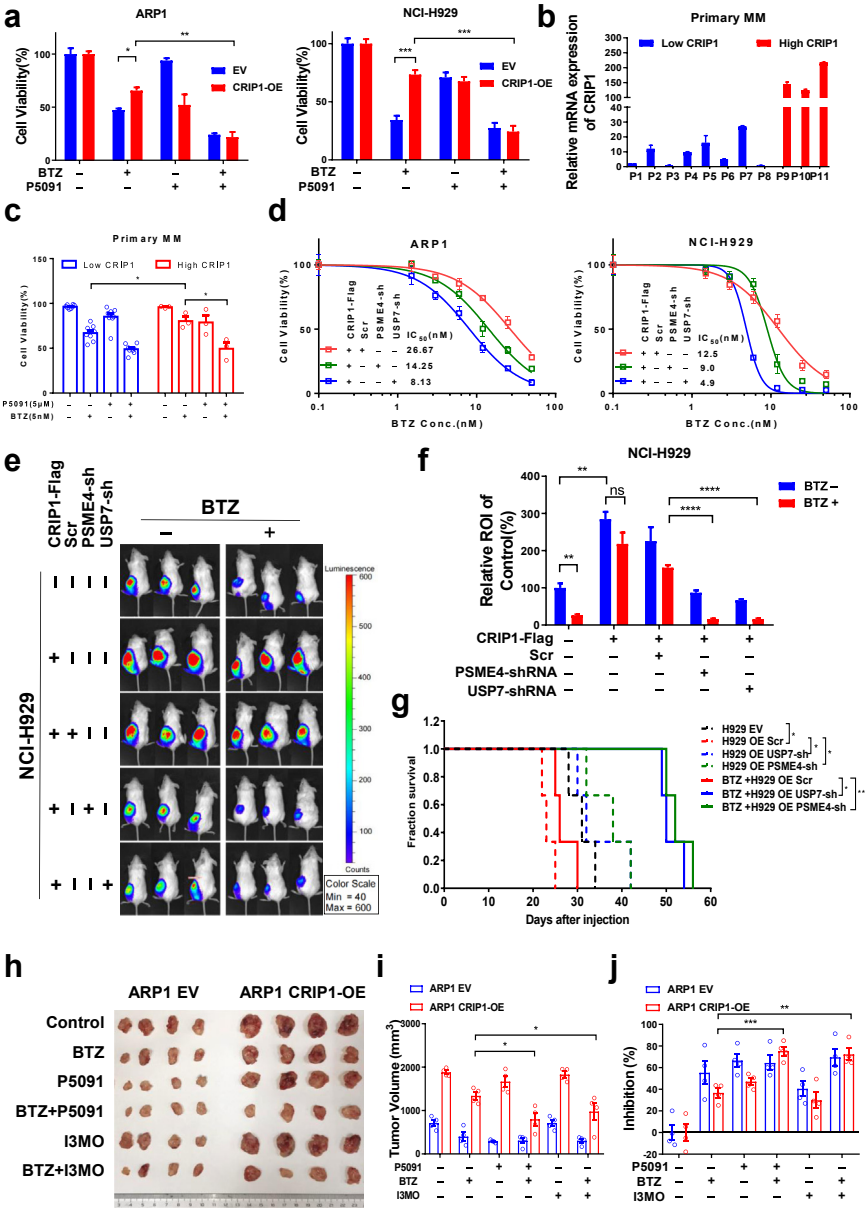

Fig. 7: **USP7 or PA200 inhibition rescues drug-resistance induced by CRIP1** (a). ARP1 and NCI-H929 cells were treated with bortezomib (10 nM), P5091 (10 μM), or a combination of both for 24 h. Cell viability was assessed using the CCK-8 assay. (b and c). qPCR was performed to detect the expression of CRIP1 in CD138+ tumour cells isolated from bone marrow aspirates of patients with MM(n = 11), and the patients with MM were divided into two groups based on the CRIP1 mRNA expression level (low CRIP1 group (n = 8) and high CRIP1 group (n = 3)). CD138+ tumour cells from patients with MM were treated with P5091 (5 μM) and/or bortezomib (5 nM) for 24 h, and cell viability was assessed using the CCK-8 assay. (d). PSME4 or USP7 was knocked down in ARP1 CRIP1-OE and NCI-H929 CRIP1-OE cells. Bortezomib was used to treat cells at concentrations ranging from 0 to 100 nM for 24 h, and the half-maximal inhibitory concentration (IC50) was calculated for each group. (e). 5 × 10^6 NCI-H929 EV, CRIP1-OE, CRIP1-OE with PSME4-shRNA, CRIP1-OE with USP7-shRNA and control cells (Scr) expressing luciferase were injected into the right flank of 7-week-old female NOD/SCID mice (n = 30, n = 3/group) to analyse tumour proliferation. After 9 days, mice were treated with bortezomib (1 mg/kg) or PBS twice weekly for 3 weeks. The tumour burden was monitored by bioluminescence imaging once the tumour volume reached 2000 mm^3. (f). The ROI values of tumours were analysed with Living Image software. (g). The survival curve of mice was plotted by euthanizing mice when tumours reached 2000 mm^3 and documenting the survival time. (h). ARP1 EV and ARP1 CRIP1-OE cells (1 × 10^6) were injected subcutaneously into the left and right flanks of NOD/SCID mice (n = 48), respectively. The mice were treated with vehicle control, bortezomib (0.5 mg/kg, i.p., twice a week from day 7), P5091 (10 mg/kg, i.p., daily from day 3), I3MO (1.25 mg/kg, i.p., three times a week from day 7), a combination of BTZ and P5091 or a combination of BTZ and I3MO. The mice were euthanized for tumour examination when the tumour volume reached 2000 mm^3. Tumour volumes were calculated using the following formula: length x $width^2$

inhibition reduced CRIP1-induced BTZ resistance in MM cells. To further verify the clinical significance of USP7 inhibition in reducing CRIP1-induced BTZ resistance, we tested the effects of P5091, alone or in combination with BTZ, on the growth of CD138-positive MM cells in primary patient samples. Primary MM cells with low levels of CRIP1 were consistently sensitive to BTZ treatment, but resistant to BTZ in primary MM cells with high levels of CRIP1. The combination treatment with P5091 significantly reversed the BTZ resistance in MM cells with high levels of CRIP1 (Fig. 7b and c). Our results demonstrated that USP7 and PA200 serve as regulators and targets of CRIP1, respectively. Therefore, we examined whether the inhibition of USP7 or PA200 could rescue the BTZ resistance induced by high levels of CRIP1. Cell viability analyses showed that MM cells were more sensitive to BTZ-induced cell growth arrest when USP7 or PA200 was knocked down in CRIP1-OE MM cell lines (Fig. 7d). An in vivo xenograft mouse model was used to confirm these effects. As shown in Fig. 7e, the knockdown of PA200 or USP7 efficiently reduced the tumour burden induced by CRIP1 overexpression. There were similar tumour sizes in the mice of the CRIP1-OE and CRIP1-OE scramble groups, which both functioned as controls in this experiment. Compared with CRIP1-OE group, the tumor burden identified by ROI in CRIP1-OE with knockdown-USP7 or-PA200 were significantly decreased (Fig. 7f, $P < 0.01$, *t* test), and the survival of tumour-bearing mice was notably prolonged (Fig. 7g, $P < 0.05$, *t* test) after BTZ treatment. These in vivo results strongly suggest that the function of CRIP1 in drug resistance can be rescued by the knockdown of USP7 or PA200.

Recently, we reported that I3MO, a proteasome inhibitor, efficiently downregulates USP7 and PA200 expression, demonstrated cytotoxicity in MM cells.[27] Herein, we examined the effects of P5091 and I3MO, alone or in combination with BTZ, on the growth of EV and CRIP1-OE MM cells in a NOD/SCID xenograft mouse model (Fig. 7h–j). Consistently, CRIP1 overexpression induced the BTZ resistance in the myeloma-bearing mouse. The combination of P5091 and I3MO significantly increased the sensitivity of MM cells to BTZ treatment. Tumour volume was significantly reduced when P5091 or I3MO was combined with BTZ treatment compared to the treatment with BTZ alone. These results further confirmed that inhibiting CRIP1 through P5091 or downregulating USP7 and PA200 through I3MO significantly rescues the drug-resistance caused by high levels of CRIP1. P5091 and I3MO are expected to become new therapeutic options for patients with high-risk MM with high CRIP1 levels.

Altogether, our study investigated the expression and regulation of CRIP1, along with its critical roles and mechanisms in PIs resistance in MM. Our findings showed that both CRIP1 and PA200 are substrates of USP7 and that CRIP1 forms a complex with USP7/PA200. CRIP1, as a scaffold protein, can facilitate the binding of USP7 to the substrate PA200, which promotes the de-ubiquitination and stabilization of PA200 mediated by USP7. CRIP1 enhances proteasome activity and autophagy through PA200, leading to survival and drug resistance in MM cells (Fig. 8). In vitro and in vivo experiments have revealed that blocking the function of CRIP1 by inhibiting the upstream USP7 and downstream substrate PA200 of CRIP1 can enhance the sensitivity of MM cells to BTZ.

Discussion

The ubiquitin-proteasome system (UPS) and autophagy lysosome system (ALP) are considered two major systems involved in proteostasis through the proteasomes and lysosomes, respectively.[44] Our findings showed that one protein, CRIP1, is involved in the two protein degradation pathways and acts as a linker between the two independent system, the UPS and ALP. CRIP1 promotes the ubiquitination and degradation of target proteins, such as Fas in CRC cells,[25] and BBOX1 in HCC cells.[26] Interestingly, we provided important evidence that CRIP1 participates in the protein ubiquitination degradation pathway in MM cells. CRIP1 enhances the deubiquitination of the proteasome activator PA200 by directly binding to USP7, resulting in the stability of PA200 in MM cells. These findings suggested that CRIP1 not only binds to E3 ligase but also to DUBs to regulate the level of protein ubiquitination and is involved in the occurrence of malignancy in diverse cellular background. Notably, in addition to protein ubiquitination, CRIP1 enhanced the proteasome activity in MM cells. These results indicated that high levels of CRIP1 participate in the occurrence and development of MM by regulating proteostasis.

The ALP is another critical pathway in protein homeostasis and involves in drug resistance to PIs.[37] Regulatory mechanisms underlying autophagy are complex. The detailed mechanisms underlying autophagy maturation and regulation in MM cells have not yet been fully elucidated. In MM, it high mobility group box protein 1 (HMGB1)-dependent autophagy can contribute to drug resistance.[45] Autophagy blockade disrupts myeloma cell recovery through proteasome

x 0.5. (i). The tumour volume was assessed in different groups of mice. (j). The inhibition rate of each group relative to the ARP1 EV or ARP1 CRIP1-OE group was calculated. The above data statistical analysis employed t-test, with the significance levels denoted as follows: * for $P < 0.05$, ** for $P < 0.01$, *** for $P < 0.001$, and **** for $P < 0.0001$.

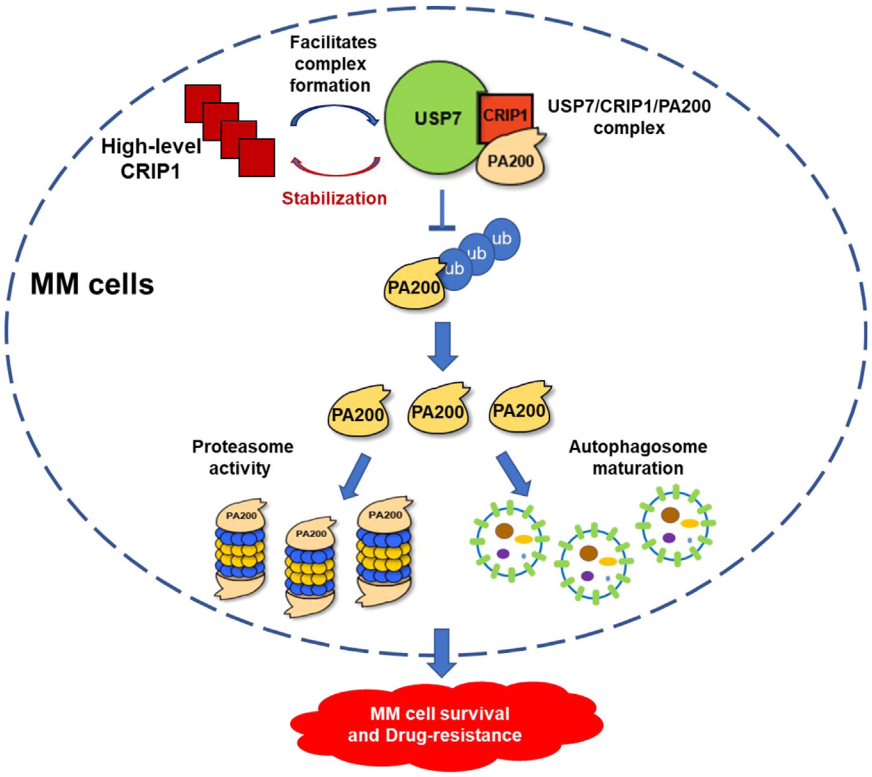

Fig. 8: **Working model of CRIP1 induces PIs resistance.**

inhibition and enhances apoptosis.[46] Strikingly, our study demonstrated that CRIP1 overexpression induced the drug-resistance to PIs depending not only on the increase in proteasome activity, but also on the maturation of autophagy.

However, the impact of CRIP1 on autophagy has not yet been reported. Our results showed that CRIP1 overexpression significantly suppressed LC3B-II degradation, efficiently promoted the autophagosomes maturation, and triggered autophagy in MM cells. Because of the direct interaction between CRIP1 and PA200, our study provides further evidence that CRIP1 promotes autophagy by the stabilization and upregulation of PA200 in MM cells. Taken together, our findings indicated that CRIP1 increases the activity of both the proteasome and autophagy by forming a complex that binds to USP7 and PA200. A study reported by S Jagannathan et al. supports our findings that knockout of PA200 inhibits the formation of aggresomes and autophagosomes.[47]

Recently, several studies reported that CRIP1 is aberrantly expressed in various solid and haematological malignancies.[18,19,24] However, the specific mechanisms underlying CRIP1 overexpression have not been fully elucidated. Recently Mao et al. reported that CRIP1 expression was regulated by the TNFα-NFκB pathway,[24] but not by the RUNX1-RUNX1T1 fusion[26] in AML cells. Our results showed that the transcription levels of CRIP1 were higher in MAF and PR (proliferation) groups, which were identified as the high-risk subgroups of MM by Zhan's study. CRIP1 protein levels were relatively higher in MM cell line with t[14,16] translocation. Therefore, cytogenetic abnormality involves in the regulation of CRIP1 expression in MM, which causes the heterogeneously increase of CRIP1 in a subset of patients with MM and associated with inferior outcomes.[32] The detailed mechanism needs to be further investigated in the future. Owing to the binding between CRIP1 and USP7, our study further clarified that CRIP1 is another substrate of USP7. USP7 is overexpressed in patients with MM[43] and stabilizes and accumulates CRIP1 in MM cells. This is the post-transcriptional regulatory mechanism underlying CRIP1 expression in MM.

Our previous study reported that the protease activator PA200 is highly expressed in patients with NDMM and RRMM and is a biomarker of poor prognosis and drug resistance in myeloma.[27] In this study, we further identified that PA200 and CRIP1 are both substrates of USP7, and that CRIP1 regulates the ubiquitination-mediated degradation of PA200 by enhancing its binding with USP7 rather than regulate PA200 at the transcription level. High levels of PA200 enhanced CRIP1-induced drug resistance, leading to MM cell proliferation. Our results indicated that CRIP1-induced resistance to PIs can be overcome by functional

suppression of CRIP1 via inhibition the activities of USP7 or PA200 by P5091 or I3MO activities.[27] Furthermore, our study provides another theoretical basis for the clinical application of P5091 or I3MO in patients with RRMM with high levels of CRIP1. Altogether, this study elucidated the critical role of CRIP1 in MM pathogenesis and identified the CRIP1/USP7/PA200 complex as a potential target for the treatment of RRMM.

CCLE data showed that CRIP1 is also overexpressed in many kinds of lymphoma and leukemia cells, including diffuse large B-cell lymphoma, acute lymphocytic leukemia and chronic lymphocytic leukemia, which suggests that high levels of CRIP1 also involved in the pathogenesis of the other B cell maligancies. However, the roles of CRIP1 in lymphocyte malignancy have not been fully understood. There were a few studies reported that CRIP1 involves the pathogenesis of acute myeloid leukemia.[48] Therefore, the functions and mechanisms underlying high levels of CRIP1 in these lymphocyte malignancies deserve further exploration.

In contrast, serveral studies reported the potential role of CRIP1 in the tumor microenvironment (TME) and the immune therapy in MM. Dang et al. has reported that CRIP1 is overexpressed in patients with RRMM who do not respond to BCMA treatment. CRIP1 reshapes the TME by increasing the secretion of vascular endothelial growth factor C (VEGFC) and C–C motif chemokine ligand 5 (CCL5) from the GC cells.[49] CRIP1 fosters MDSC trafffcking via facilitating NF-κB/p65 nuclear translocation in pancreatic ductal adenocarcinoma.[50]

In summary, this study reported the pivotal roles and underlying mechanisms of CRIP1 in the pathogenesis of MM. CRIP1 plays a critical role in PIs resistance in MM by binding to USP7 and PA200. Our findings provide a perspective on the CRIP1/USP7/PA200 complex formation in the ubiquitin-dependent proteasome degradation and autophagy maturation involved in the progression of MM. CRIP1 promotes proteasome activity and autophagosome maturation in MM cells by stabilizing PA200. High-level CRIP1 is a biomarker for patients with high-risk myeloma who would benefit from adjuvant therapy targeting USP7 or PA200.

Contributors

TPX and YZ contributed equally to this work, conducting experiments, acquiring data, analyzing data, and writing the manuscript. HM designed the research studies. SH contributed to data collection and data analyses. LLT constructed the animal model. SXY, XZS participated in sample collection. YZ, HM and QLG contributed to the literature search and manuscript revision. All authors contributed to data acquisition and data interpretation, and all authors reviewed and approved the final version of the manuscript. The corresponding author attests that all listed authors meet authorship criteria and that no others meeting the criteria have been omitted. TPX, YZ and HM have verified the underlying data.

Data sharing statement

All original sequencing data sets of the cell line are deposited in the NCBI Gene Expression Omnibus database (GSE248339).

Declaration of interests

The authors have declared that no conflicts of interest exist.

Acknowledgements

This research was funded by the National Natural Science Foundation of China (82370210, 82170194, 81920108006 and 82270175), the CAMS Innovation Fund for Medical Sciences (CIFMS 2021-I2M-1-040 and CIFMS 2022-I2M-1-022), and the Natural Science Foundation of Fujian Province of China (2021J02040).

Appendix A. Supplementary data

Supplementary data related to this article can be found at https://doi.org/10.1016/j.ebiom.2023.104961.

References

1 van de Donk N, Pawlyn C, Yong KL. Multiple myeloma. *Lancet*. 2021;397(10272):410–427.
2 Zhao L, Zhao J, Zhong K, Tong A, Jia D. Targeted protein degradation: mechanisms, strategies and application. *Signal Transduct Target Ther*. 2022;7(1):113.
3 Hanley SE, Cooper KF. Sorting nexins in protein homeostasis. *Cells*. 2020;10(1):17.
4 Hao M, Franqui-Machin R, Xu H, et al. NEK2 induces osteoclast differentiation and bone destruction via heparanase in multiple myeloma. *Leukemia*. 2017;31(7):1648–1650.
5 Hao M, Zhang L, An G, et al. Suppressing miRNA-15a/-16 expression by interleukin-6 enhances drug-resistance in myeloma cells. *J Hematol Oncol*. 2011;4:37.
6 Dikic I. Proteasomal and autophagic degradation systems. *Annu Rev Biochem*. 2017;86:193–224.
7 Pohl C, Dikic I. Cellular quality control by the ubiquitin-proteasome system and autophagy. *Science*. 2019;366(6467):818–822.
8 Lee S, Jeon YM, Cha SJ, et al. PTK2/FAK regulates UPS impairment via SQSTM1/p62 phosphorylation in TARDBP/TDP-43 proteinopathies. *Autophagy*. 2020;16(8):1396–1412.
9 Ballabio A, Bonifacino JS. Lysosomes as dynamic regulators of cell and organismal homeostasis. *Nat Rev Mol Cell Biol*. 2020;21(2):101–118.
10 Franqui-Machin R, Hao M, Bai H, et al. Destabilizing NEK2 overcomes resistance to proteasome inhibition in multiple myeloma. *J Clin Invest*. 2018;128(7):2877–2893.
11 Dimopoulos MA, Richardson PG, Moreau P, Anderson KC. Current treatment landscape for relapsed and/or refractory multiple myeloma. *Nat Rev Clin Oncol*. 2015;12(1):42–54.
12 Hao M, Zang M, Wendlandt E, et al. Low serum miR-19a expression as a novel poor prognostic indicator in multiple myeloma. *Int J Cancer*. 2015;136(8):1835–1844.
13 Wei X, Yu Z, Tang P, et al. Multiple myeloma-derived miR-27b-3p facilitates tumour progression via promoting tumour cell proliferation and immunosuppressive microenvironment. *Clin Transl Med*. 2023;13(1):e1140.
14 Ito S. Proteasome inhibitors for the treatment of multiple myeloma. *Cancers (Basel)*. 2020;12(2):265.
15 Narayanan S, Cai CY, Assaraf YG, et al. Targeting the ubiquitin-proteasome pathway to overcome anti-cancer drug resistance. *Drug Resist Updat*. 2020;48:100663.
16 Mogollón P, Díaz-Tejedor A, Algarín EM, Paíno T, Garayoa M, Ocio EM. Biological background of resistance to current standards of Care in multiple myeloma. *Cells*. 2019;8(11):1432.
17 Lv J, Sun H, Gong L, et al. Aberrant metabolic processes promote the immunosuppressive microenvironment in multiple myeloma. *Front Immunol*. 2022;13:1077768.
18 He G, Zou L, Zhou L, Gao P, Qian X, Cui J. Cysteine-rich intestinal protein 1 silencing inhibits migration and invasion in human colorectal cancer. *Cell Physiol Biochem*. 2017;44(3):897–906.
19 Lambropoulou M, Deftereou TE, Kynigopoulos S, et al. Co-expression of galectin-3 and CRIP-1 in endometrial cancer: prognostic value and patient survival. *Med Oncol*. 2016;33(1):8.
20 Ludyga N, Englert S, Pflieger K, et al. The impact of cysteine-rich intestinal protein 1 (CRIP1) in human breast cancer. *Mol Cancer*. 2013;12:28.
21 Sun H, Zhou R, Zheng Y, et al. CRIP1 cooperates with BRCA2 to drive the nuclear enrichment of RAD51 and to facilitate homologous repair upon DNA damage induced by chemotherapy. *Oncogene*. 2021;40(34):5342–5355.

22 Cousins RJ, Lanningham-Foster L. Regulation of cysteine-rich intestinal protein, a zinc finger protein, by mediators of the immune response. *J Infect Dis*. 2000;182(Suppl 1):S81–S84.
23 Xia S, Li X, Xu S, Ni X, Zhan W, Zhou W. Sublethal heat treatment promotes breast cancer metastasis and its molecular mechanism revealed by quantitative proteomic analysis. *Aging (Albany NY)*. 2022;14(3):1389–1406.
24 Gao Y, Li JY, Mao JY, Zhou JF, Jiang L, Li XP. Comprehensive analysis of CRIP1 expression in acute myeloid leukemia. *Front Genet*. 2022;13:923568.
25 Zhang L, Zhou R, Zhang W, et al. Cysteine-rich intestinal protein 1 suppresses apoptosis and chemosensitivity to 5-fluorouracil in colorectal cancer through ubiquitin-mediated Fas degradation. *J Exp Clin Cancer Res*. 2019;38(1):120.
26 Wang J, Zhou Y, Zhang D, et al. CRIP1 suppresses BBOX1-mediated carnitine metabolism to promote stemness in hepatocellular carcinoma. *EMBO J*. 2022;41(15):e110218.
27 Yu Z, Wei X, Liu L, et al. Indirubin-3'-monoxime acts as proteasome inhibitor: therapeutic application in multiple myeloma. *eBioMedicine*. 2022;78:103950.
28 Zhuang J, Shirazi F, Singh RK, et al. Ubiquitin-activating enzyme inhibition induces an unfolded protein response and overcomes drug resistance in myeloma. *Blood*. 2019;133(14):1572–1584.
29 Wang Q, Zhao D, Xian M, et al. MIF as a biomarker and therapeutic target for overcoming resistance to proteasome inhibitors in human myeloma. *Blood*. 2020;136(22):2557–2573.
30 Yu T, Du C, Ma X, et al. Polycomb-like protein 3 induces proliferation and drug resistance in multiple myeloma and is regulated by miRNA-15a. *Mol Cancer Res*. 2020;18(7):1063–1073.
31 Li Z, Liu L, Du C, et al. Therapeutic effects of oligo-single-stranded DNA mimicking of hsa-miR-15a-5p on multiple myeloma. *Cancer Gene Ther*. 2020;27(12):869–877.
32 Zhan F, Huang Y, Colla S, et al. The molecular classification of multiple myeloma. *Blood*. 2006;108(6):2020–2028.
33 Bianchi G, Oliva L, Cascio P, et al. The proteasome load versus capacity balance determines apoptotic sensitivity of multiple myeloma cells to proteasome inhibition. *Blood*. 2009;113(13):3040–3049.
34 Obeng EA, Carlson LM, Gutman DM, Harrington WJ Jr, Lee KP, Boise LH. Proteasome inhibitors induce a terminal unfolded protein response in multiple myeloma cells. *Blood*. 2006;107(12):4907–4916.
35 Jung S, Jeong H, Yu SW. Autophagy as a decisive process for cell death. *Exp Mol Med*. 2020;52(6):921–930.
36 Lu Z, Xu N, He B, et al. Inhibition of autophagy enhances the selective anti-cancer activity of tigecycline to overcome drug resistance in the treatment of chronic myeloid leukemia. *J Exp Clin Cancer Res*. 2017;36(1):43.
37 Zamame Ramirez JA, Romagnoli GG, Kaneno R. Inhibiting autophagy to prevent drug resistance and improve anti-tumor therapy. *Life Sci*. 2021;265:118745.
38 Chang H, Zou Z. Targeting autophagy to overcome drug resistance: further developments. *J Hematol Oncol*. 2020;13(1):159.
39 Hwang HJ, Kim YK. The role of LC3B in autophagy as an RNA-binding protein. *Autophagy*. 2023;19(3):1028–1030.
40 Vogl DT, Stadtmauer EA, Tan KS, et al. Combined autophagy and proteasome inhibition: a phase 1 trial of hydroxychloroquine and bortezomib in patients with relapsed/refractory myeloma. *Autophagy*. 2014;10(8):1380–1390.
41 Xia J, He Y, Meng B, et al. NEK2 induces autophagy-mediated bortezomib resistance by stabilizing Beclin-1 in multiple myeloma. *Mol Oncol*. 2020;14(4):763–778.
42 Lu Y, Wang Y, Xu H, Shi C, Jin F, Li W. Profilin 1 induces drug resistance through Beclin1 complex-mediated autophagy in multiple myeloma. *Cancer Sci*. 2018;109(9):2706–2716.
43 Chauhan D, Tian Z, Nicholson B, et al. A small molecule inhibitor of ubiquitin-specific protease-7 induces apoptosis in multiple myeloma cells and overcomes bortezomib resistance. *Cancer Cell*. 2012;22(3):345–358.
44 Hetz C, Zhang K, Kaufman RJ. Mechanisms, regulation and functions of the unfolded protein response. *Nat Rev Mol Cell Biol*. 2020;21(8):421–438.
45 Bashiri H, Tabatabaeian H. Autophagy: a potential therapeutic target to tackle drug resistance in multiple myeloma. *Int J Mol Sci*. 2023;24(7):6019.
46 Moriya S, Komatsu S, Yamasaki K, et al. Targeting the integrated networks of aggresome formation, proteasome, and autophagy potentiates ER stress-mediated cell death in multiple myeloma cells. *Int J Oncol*. 2015;46(2):474–486.
47 Jagannathan S, Vad N, Vallabhapurapu S, Vallabhapurapu S, Anderson KC, Driscoll JJ. MiR-29b replacement inhibits proteasomes and disrupts aggresome+autophagosome formation to enhance the antimyeloma benefit of bortezomib. *Leukemia*. 2015;29(3):727–738.
48 Deng X, Zeng Y, Qiu X, et al. CRIP1 supports the growth and migration of AML-M5 subtype cells by activating Wnt/β-catenin pathway. *Leuk Res*. 2023;130:107312.
49 Wu Z, Qu B, Yuan M, et al. CRIP1 reshapes the gastric cancer microenvironment to facilitate development of lymphatic metastasis. *Adv Sci (Weinh)*. 2023;10:e2303246.
50 Liu X, Tang R, Xu J, et al. CRIP1 fosters MDSC trafficking and resets tumour microenvironment via facilitating NF-κB/p65 nuclear translocation in pancreatic ductal adenocarcinoma. *Gut*. 2023;72(12):2329–2343.